Polymer Chemistry

PAPER

View Article Online
View Journal | View Issue

Cite this: *Polym. Chem.*, 2016, **7**, 6211

Structurally defined nanographene-containing conjugated polymers for high quality dispersions and optoelectronic applications†

Po-I. Wang,[a] Wojciech Pisula,[b] Klaus Müllen*[b] and Der-Jang Liaw*[a]

Received 30th July 2016,
Accepted 13th September 2016

DOI: 10.1039/c6py01330a

www.rsc.org/polymers

Novel conjugated polymers such as poly(phenylene-fluorene) **P1** and poly(triphenylbenzene-fluorene) **P2** with hexaphenylbenzene (HPB) as a pending side group were prepared by Suzuki coupling using the dibromo monomers **M1** and **M2** with 9,9-dioctylfluorene-2,7-diboronic acid bis(1,3-propanediol) ester, respectively. The HPB moiety of **P1** and **P2** can be oxidatively cyclodehydrogenated with $FeCl_3$ in nitromethane, yielding polymers **P3** and **P4** with hexa-*peri*-hexabenzocoronene (*i.e.*, nanographene) units. The cyclodehydrogenation of nanographene-containing polymers was confirmed by FT-IR spectroscopy. In addition, X-ray powder diffraction of both **P3** and **P4** revealed a polymer interlayer spacing of 1.3 nm being dominated by the nanographenes. The glass transition temperatures (T_gs) of **P1** and **P2** were 202 °C and 235 °C, respectively, while both **P3** and **P4** with nanographenes possessed T_gs higher than 300 °C. Compared to **P3**, **P4** with a triphenylbenzene moiety in its backbone can be well dispersed without aggregation in *N*-cyclohexyl-2-pyrrolidone (CHP), as confirmed by UV-Vis spectroscopy, photoluminescence spectroscopy (PL) and photoluminescence-excitation (PLE) maps.

Introduction

Graphene is a two-dimensional sheet consisting of six-membered rings of sp^2-hybridized carbon atoms. Due to its long-range π-conjugation, graphene possesses extraordinary thermal, mechanical and electrical properties.[1,2] The methods of preparation of graphene can be divided into two classes; a top-down approach starting from complex precursors or graphite structures, or a bottom-up approach using polycyclic aromatic hydrocarbons (PAHs) as simple building blocks. PAHs can be linked together to obtain larger sheets with the potential advantage of controlling the dimensions of the resulting graphene sheets on nanometer or even micrometer scales. PAHs are one of the most widely investigated classes of compounds in organic synthetic chemistry and materials science.[3] PAHs can be further classified by the type of ring connectivity, as in *kata*- and *peri*-condensed hydrocarbons.[4] The former consists of benzenoid rings in linear or angular arrangements such as anthracene, tetracene, phenanthrene or tetraphene. *peri*-Condensed polyarenes are another major class of PAHs, examples of which are pyrene, ovalene and hexa-*peri*-hexabenzocoronenes (HBCs).

Hexa-*peri*-hexabenzocoronenes (HBCs) are an example of PAHs and have the chemical formula $C_{42}H_{18}$. The first synthesis of HBCs was performed using dibenzo-*peri*-naphthene by Erich Clar and coworkers in 1958. Halleux *et al.* and Schmidt *et al.* have reported different routes for synthesizing HBCs through the cyclization of precursors. However, all methods of synthesizing HBCs give low yields and require complicated workups.[5] Therefore, Müllen and coworkers developed an efficient way to prepare HBCs through Scholl-type intramolecular oxidative cyclodehydrogenation by treating hexaphenylbenzene (HPB) with $Cu(OTf)_2/AlCl_3$ in CS_2, or $FeCl_3$ dissolved in nitromethane.[6] This method has been used for the preparation of complex PAHs with different sizes and shapes.[7] In recent years, HBCs and their derivatives have attracted attention due to their high symmetry, high stability, high charge carrier mobility and self-assembly. HBCs and their derivatives have been widely used in synthetic chemistry, liquid crystalline mesophases and optoelectronics.[8–10] HBCs have been considered "nano-graphene" or "super-benzene" due to their large π-system with 13 benzenes and D_{6h}-symmetry. HBCs can also be considered a prototype for giant and planar PAHs including $C_{222}H_{42}$, $C_{474}H_{66}$, and graphene nano-

[a]*Department of Chemical Engineering, National Taiwan University of Science and Technology, 10607 Taipei, Taiwan. E-mail: liawdj@gmail.com, liawdj@mail.ntust.edu.tw; Fax: +886-2-23781441, +886-2-27376644; Tel: +886-2-27376638, +886-2-27335050*

[b]*Max Planck Institute for Polymer Research, Ackermannweg 10, 55128 Mainz, Germany. E-mail: muellen@mpip-mainz.mpg.de; Fax: +49 6131 379 350; Tel: +49 6131 379 150*

† Electronic supplementary information (ESI) available: Characterization details such as NMR spectra, the MALDI-TOF MS spectrum and UV-Vis absorption spectra for the monomers or conjugated polymers. See DOI: 10.1039/c6py01330a

ribbons. However, these planar hydrocarbons are generally insoluble in common solvents as a result of their strong π–π stacking interactions. To enhance the solubility of HBCs, peripheral alkyl groups should be incorporated.[11] These HBC derivatives with substituents can be cast into films through a solution process and used for applications such as organic light-emitting diodes, organic photovoltaics and thin film transistors.[12]

For reasons of atom economy and to broaden the scope of the synthesis of various HBC materials, non-substituted HBCs carry the great advantage of their simple synthesis. The thermal properties and carrier mobility of HBCs will not be affected by aliphatic alkyl chains. The unsubstituted HBC dispersion *via* ultrasonic agitation was found to be an efficient method both in organic solvents and in aqueous surfactant solution, but aggregation phenomena of HBCs were observed when HBCs were dispersed in poor solvents or unsuitable surfactant systems.[13,14] As reported by Coleman *et al.*, amide solvents such as cyclohexylpyrrolidone (CHP) perform well when dispersing single-walled carbon nanotubes (SWCNTs) and graphenes.[15] The dispersion of HBC derivatives was limited to the selection of an amide solvent or a specific surfactant in an aqueous solvent. Therefore, we demonstrate the dispersion of a conjugated polymer bearing a HBC moiety to improve the dispersibility in various organic solvents.

In this study, the conjugated polymers **P1** and **P2** were synthesized from a dibromo monomer with a non-substituted HPB unit and a diboronic ester monomer of dioctyl-fluorene (Scheme 1). The solubility of the polymer is enhanced by the addition of flexible fluorene alkyl-chains, and premature precipitation during polymerization is avoided. In addition, HPB can be regarded as a precursor of HBCs, and the conjugated polymers **P3** and **P4** with a HBC moiety can be prepared by a Scholl reaction. To confirm cyclodehydrogenation, **P1–P4** were studied using FT-IR spectroscopy and X-ray powder diffraction to identify HPB and HBC units. To the best of our knowledge, exfoliation of the HBC-containing conjugated polymer has not been reported yet. We prepared dispersions of **P3** and **P4** for spectroscopic characterization using UV-Vis spectroscopy, PL spectroscopy and photoluminescence-excitation (PLE) maps.

Experimental

Materials

(4-Bromophenyl)pentaphenylbenzene (**1**) was prepared *via* Diels–Alder cycloaddition according to a procedure reported by Müllen *et al.*[16] 1,3,5-Tri(4-bromophenyl)benzene was synthesized by the cyclocondensation of *p*-bromoacetophenone.[17] 4-Bromoiodobenzene, copper iodide (CuI), diphenyl ether,

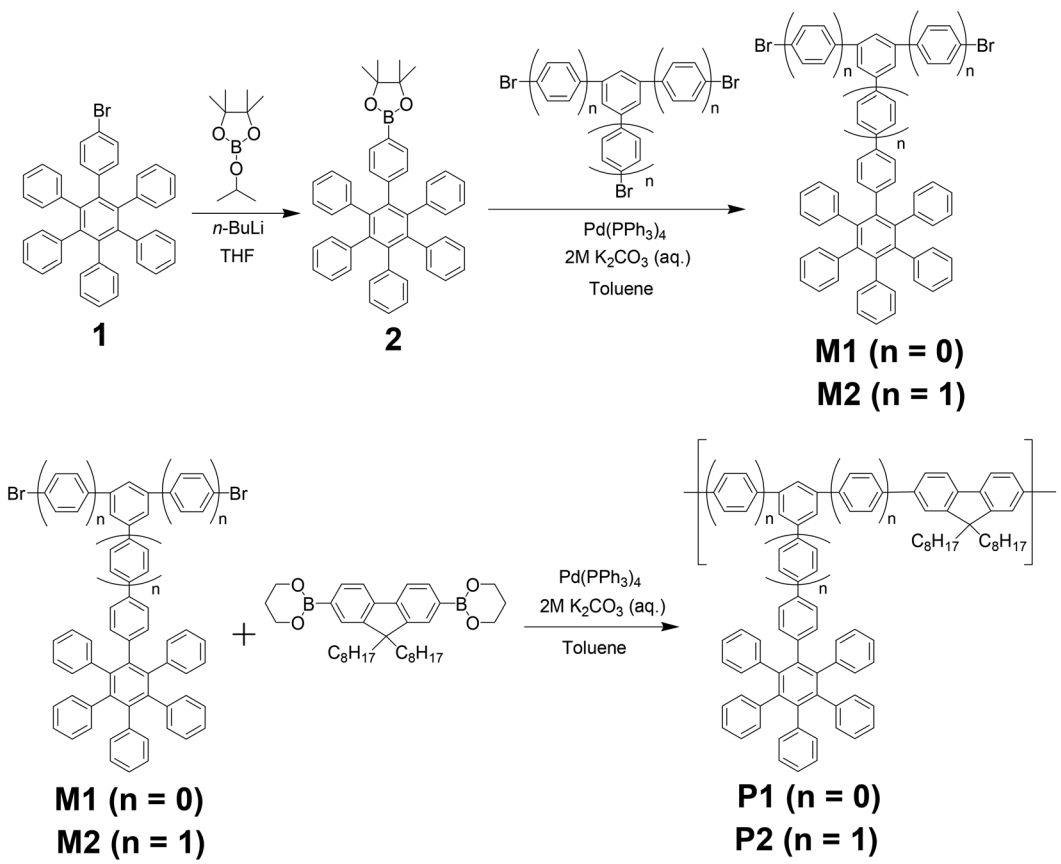

Scheme 1 The synthesis of HPB-containing monomers **M1** and **M2** as well as conjugated polymers **P1** and **P2**.

iron(III) chloride ($FeCl_3$), phenylacetylene, piperidine, 7,7,8,8-tetracyanoquinodimethane (TCNQ) and tetrakis(triphenylphosphine)palladium(0) ($Pd(PPh_3)_4$) were purchased from Acros Organics. Anhydrous potassium carbonate (K_2CO_3) was purchased from Fisher Chemical. 9,9-Dioctylfluorene-2,7-diboronic acid bis(1,3-propanediol) ester, *n*-butyllithium solution (2.5 M in hexanes), 2-isopropoxy-4,4,5,5-tetramethyl[1,3,2] dioxaborolane, *p*-bromoacetophenone and tetraphenylcyclopentadienone were purchased from Sigma-Aldrich Chemical Co. The solvents (analytical grade) were purchased from Merck. Tetrahydrofuran and toluene were distilled from sodium/benzophenone (deep purple) under nitrogen before use. All other reagents were used as received.

Measurements

IR spectra were recorded in the range 400–4200 cm^{-1} for synthesized monomers and polymers in a KBr disk (Bio-Rad Digilab FTS-3500). NMR spectra were recorded using a Bruker Avance III HD-600 (^1H at 600 MHz and ^{13}C at 150 MHz). Differential scanning calorimetric analysis was performed on a differential scanning calorimeter (TA Instrument TA 910) under nitrogen at a flow rate of 50 cm^3 min^{-1} and a heating rate of 10 K min^{-1}. Thermogravimetric analysis was performed on a TA Instrument Dynamic TGA 2950 under nitrogen at a flow rate of 30 cm^3 min^{-1} and a heating rate of 10 K min^{-1}. X-ray diffraction experiments were performed using a Bruker D8 X-ray powder diffractometer (Cu-Kα: 0.15406 nm) at a scanning rate of 0.1° per 20 s. Mass spectra were obtained using a Bruker micro TOF-QII and MALDI-TOF MS spectra were characterized by using a BrukerAutoflex III TOF/TOF (using TCNQ as a matrix). Weight-average (M_w) and number-average (M_n) molecular weights were determined by gel permeation chromatography (GPC). Four Waters (Ultrastyragel) columns (300 × 7.5 mm, guard, 105, 104, 103, and 500 Å in a series) were used for GPC analysis with tetrahydrofuran (THF; 1 mL min^{-1}) as the eluent. The eluents were monitored with a UV detector (JMST Systems, VUV-24, USA) at 254 nm, and polystyrene was used as the standard. The UV-Vis absorption spectra of the specimens were recorded on a JASCO V-670 spectrophotometer at room temperature in air. Photoluminescence (PL) spectra and photoluminescence-excitation (PLE) maps were obtained using a HORIBA JOBIN FluoroMax-3 with a 1 cm × 1 cm quartz cuvette. The photoluminescence quantum yield (Φ_{PL}) values of the samples in dilute THF solution were measured in an integrating sphere using 9,10-diphenylanthracence in cyclohexane as a reference (Φ_{PL} = 0.9). A cyclic voltammeter (CV; CHI model 619A) was used to measure oxidative potentials with a standard three-electrode electrochemical cell in an acetonitrile solution containing 0.1 M tetrabutylammoniumperchlorate (TBAP) at room temperature under argon (scanning rate = 0.1 V s^{-1}).

Synthesis of 4-(4,4,5,5-tetramethyl-1,3,2-dioxaborolan-2-yl-phenyl)pentaphenylbenzene (2)

To a solution of (4-bromophenyl)pentaphenylbenzene (**1**) (1 g, 1.63 mmol) in anhydrous THF (150 mL) under nitrogen at −78 °C, *n*-butyllithium (2.5 M in hexane, 1.3 mL, 3.26 mmol) was added and stirred at −78 °C for 30 min. 2-Isopropoxy-4,4,5,5-tetramethyl-[1,3,2]dioxaborolane (0.91 g, 4.89 mmol) was added at −78 °C, and the resulting solution was stirred at room temperature for 6 h. Water (5 mL) was added to quench the reaction, followed by solvent removal using a rotary evaporator. The crude products were dissolved in dichloromethane (50 mL), extracted with brine (30 mL × 3), dried with $MgSO_4$ and concentrated in a vacuum. The residue was purified by column chromatography (silica gel, *n*-hexane/CH_2Cl_2 = 3/1) to obtain white powders (0.75 g, yield = 70%). IR (KBr): 4050 cm^{-1}, 3078 cm^{-1}, 3051 cm^{-1} and 3022 cm^{-1} (Ar–H stretch), 2978 cm^{-1}, 2929 cm^{-1}, and 2864 cm^{-1} (C–H stretch), 1614 cm^{-1}, 1598 cm^{-1} and 1494 cm^{-1} (C=C stretch in Ar), 696 cm^{-1}. ^1H NMR (600 MHz, CD_2Cl_2, Me_4Si): δ (ppm) = 1.25 (s, 12H, H_c), 6.84–6.89 (m, 25H, phenyl-H), 6.90 (d, 2H, J = 8.4 Hz, H_a), 7.22 (d, 2H, J = 7.8 Hz, H_b); ^{13}C NMR (150 MHz, CD_2Cl_2, Me_4Si): δ (ppm) = 25.29 (C_3), 84.20 (C_6), 125.75, 125.84, 127.06, 127.13, 131.36 (C_1), 131.92, 133.42 (C_2), 140.63 (C_5), 140.71, 140.96, 141.19, 141.28, 141.31, 144.38 (C_4).

Synthesis of 4′-(1,3-dibromophenyl)hexaphenylbenzene (M1)

Compound (**2**) (0.6 g, 0.91 mmol), tribromobenzene (0.31 g, 1 mmol), and $Pd(PPh_3)_4$ (23 mg, 0.02 mmol) were dissolved in degassed toluene (10 mL) and added to a three-neck round-bottom flask with a condenser. Then, 2 M aqueous solution of K_2CO_3 (8 mL) was added. The mixture was vigorously stirred at 105 °C for 12 h under flowing nitrogen. After cooling, the resulting mixture was extracted with toluene/water twice, after which the organic layer was separated and concentrated using a rotary evaporator. The residue was purified by column chromatography (silica gel, *n*-hexane/CH_2Cl_2 = 4/1) to produce white powders (0.42 g, yield = 60%). IR (KBr): 4054 cm^{-1}, 3078 cm^{-1}, 3059 cm^{-1} and 3024 cm^{-1} (Ar–H stretch), 1600 cm^{-1}, 1581 cm^{-1} and 1539 cm^{-1} (C=C stretch in Ar), 698cm^{-1}. ^1H NMR (600 MHz, $CDCl_3$, Me_4Si): δ (ppm) = 6.82–6.90 (m, 25H, phenyl-H), 6.92 (d, 2H, J = 8.4 Hz, H_a), 7.05 (d, 2H, J = 8.4 Hz, H_b), 7.50 (s, 2H, H_c), 7.53 (s, 1H, H_d). ^{13}C NMR (150 MHz, CD_2Cl_2, Me_4Si): δ (ppm) = 123.03 (C_8), 125.10 (C_2), 125.24, 125.36, 126.60, 126.72, 128.53 (C_3), 131.38, 132.07 (C_4), 132.10 (C_1), 134.56 (C_6), 139.44, 140.27, 140.42, 140.47, 140.50, 140.62, 141.27(C_5), 144.38 (C_7).

Synthesis of 4′-[5,7-bis(4-bromophenyl)biphenyl] hexaphenylbenzene (M2)

The title compound (**M2**) was prepared in a manner analogous to the procedure of **M1** to obtain the product as white powders (yield = 65%). IR (KBr): 4054 cm^{-1}, 3080 cm^{-1}, 3055 cm^{-1} and 3024 cm^{-1} (Ar–H stretch), 1598 cm^{-1} and 1489 cm^{-1} (C=C stretch in Ar), 1072 cm^{-1} (Ar–Br), 698 cm^{-1}. ^1H NMR (600 MHz, $CDCl_3$, Me_4Si): δ (ppm) = 6.85–6.92 (m, 25H, phenyl-H), 6.94 (d, 2H, J = 8.4 Hz, H_a), 7.21 (d, 2H, J = 8.4 Hz, H_b), 7.54 (d, 4H, J = 8.4 Hz, H_g), 7.56 (d, 2H, J = 8.4 Hz, H_c), 7.61 (d, 4H, J = 8.4 Hz, H_h), 7.64 (d, 2H, J = 7.8 Hz, H_d), 7.67 (s, 1H, H_f), 7.73 (s, 2H, H_e); ^{13}C NMR (150 MHz, CD_2Cl_2, Me_4Si): δ (ppm) = 121.97 (C_{16}), 124.59 (C_6), 125.01(C_2 + C_5), 125.21,

125.25, 126.59, 126.68, 127.14 (C_3), 127.42 (C_4), 128.90 (C_7), 131.42, 131.45, 131.96 (C_1), 131.99 (C_8), 136.60 (C_{10}), 139.12 (C_{12}), 139.82 (C_{15}), 140.13 (C_{11}), 140.20 (C_9), 140.35, 140.43, 140.48, 140.58, 141.34 (C_{14}), 142.23 (C_{13}).

Synthesis of poly[4′-(1,3-phenyl)]hexaphenylbenzene-*alt*-2,7-(9,9-dioctylfluorene) (P1) *via* Suzuki coupling

The dibromo monomer (**M1**) (0.2093 g, 0.273 mmol), 9,9-dioctylfluorene-2,7-diboronic acid bis(1,3-propanediol) ester (0.1522 g, 0.273 mmol), and $Pd(PPh_3)_4$ (6.3 mg, 0.05 mmol) were dissolved in degassed toluene (10 mL) and added to a three-neck round-bottom flask with a condenser and a 2 M aqueous solution of K_2CO_3 (8 mL). The resulting solution was stirred at 105 °C for 48 h under the flow of nitrogen. After cooling, the solution was extracted with toluene/water twice to remove the base. The organic layer was separated, concentrated by using a rotary evaporator and precipitated in excess methanol. The grey fibrous product was filtered and purified by Soxhlet extraction with acetone for 48 h (0.25 g, yield = 92%). IR (KBr): 4046 cm^{-1}, 3078 cm^{-1}, 3055 cm^{-1} and 3028 cm^{-1} (Ar–H stretch), 2955 cm^{-1}, 2924 cm^{-1} and 2854 cm^{-1} (C–H stretch), 1597 cm^{-1} and 1496 cm^{-1} (C=C stretch in Ar), 748 cm^{-1}, 698 cm^{-1}. ^{1}H NMR (600 MHz, $CDCl_3$, Me_4Si): δ (ppm) = 0.70–0.92 (m, 10H, H_i, H_o), 1.02–1.22 (m, 16H, H_j, H_k, H_l, H_m), 1.19 (m, 4H, H_n), 2.09 (s, 4H, H_h), 6.75–6.92 (m, 25H, phenyl-H), 6.98 (d, 2H, H_a), 7.35 (d, 2H, H_b), 7.54 (2H, H_c), 7.63 (2H, H_g), 7.68 (2H, H_e), 7.74 (1H, H_d), 7.81 (2H, H_f); ^{13}C NMR (150 MHz, $CDCl_3$, Me_4Si): δ (ppm) = 14.04 (C_{15}), 22.57 (C_{14}), 23.87 (C_9), 29.18 (C_{11} + C_{12}), 30.02 (C_{10}), 31.72 (C_{13}), 40.43 (C_8), 55.45 (C_{23}), 119.39, 120.04 (C_6), 121.60 (C_7), 124.53 (C_4), 124.82 (C_3), 125.04 (C_2), 125.21, 126.15 (C_5), 126.59, 126.69, 127.85, 131.11, 131.43, 132.02 (C_1), 137.25 (C_{17}), 140.16, 140.37, 140.48, 140.60 (C_{16} + C_{18} + C_{19} + C_{20}), 151.90 (C_{22}). M_n = 21 400 g mol^{-1} and PDI = 1.34 by GPC.

Synthesis of poly[4′-(5,7-(4,4-diphenyl)biphenyl)] hexaphenylbenzene-*alt*-2,7-(9,9-dioctylfluorene) (P2) *via* Suzuki coupling

The title compound (**P2**) was prepared in a manner analogous to the procedure of **P1** to obtain a grey fibrous product (yield = 90%). IR (KBr): 4042 cm^{-1}, 3080 cm^{-1}, 3055 cm^{-1} and 3026 cm^{-1} (Ar–H stretch), 2949 cm^{-1}, 2920 cm^{-1} and 2848 cm^{-1} (C–H stretch), 1585 cm^{-1} and 1502 cm^{-1} (C=C stretch in Ar), 748 cm^{-1}, 696 cm^{-1}. ^{1}H NMR (600 MHz, $CDCl_3$, Me_4Si): δ (ppm) = 0.78–0.85 (m, 10H, H_m, H_s), 1.07–1.18 (m, 16H, H_n, H_o, H_p, H_q), 1.21 (m, 4H, H_r), 2.11 (s, 4H, H_l), 6.82–6.93 (m, 25H, phenyl-H), 6.95 (d, 2H, J = 7.8 Hz, H_a), 7.25 (d, 2H, J = 8.4 Hz, H_b), 7.63 (d, 2H, J = 8.4 Hz, H_c), 7.67 (s, 2H, H_k), 7.71 (d, 2H, J = 8.4 Hz, H_i), 7.75 (d, 2H, J = 7.8 Hz, H_d), 7.81–7.88 (m, 10H, H_g, H_h, H_j), 7.89 (s, 2H, H_e), 7.93 (s, 1H, H_f); ^{13}C NMR (150 MHz, $CDCl_3$, Me_4Si): δ (ppm) = 14.06 (C_{19}), 22.59 (C_{18}), 23.87 (C_{13}), 29.20 (C_{15} + C_{16}), 30.04 (C_{14}), 31.78 (C_{17}), 40.48 (C_{12}), 55.36 (C_{31}), 120.14 (C_{10}), 121.49 (C_{11}), 125.04 (C_6), 125.21 (C_5), 125.26 (C_2), 126.02 (C_9), 126.59, 126.69, 127.17 (C_3), 127.20, 127.39, 127.53 (C_4), 127.67 (C_8), 127.77 (C_7), 128.77, 131.44, 131.47, 131.97 (C_1), 136.72 (C_{21}), 139.53 (C_{28}), 139.64 (C_{23}), 139.91 (C_{20} + C_{22} + C_{26}), 140.08 (C_{27}), 140.25 (C_{29}), 140.38, 140.43, 140.60, 140.99 (C_{24}), 142.09 (C_{25}), 151.83 (C_{30}). M_n = 24 900 g mol^{-1} and PDI = 1.94 by GPC.

Synthesis of poly[4′-(1,3-phenyl)]hexabenzocoronene-*alt*-2,7-(9,9-dioctylfluorene) (P3) *via* cyclodehydrogenation

A total of 36 equivalents of iron(III) chloride in nitromethane (300 mg mL^{-1}) per hexaphenylbenzene unit were added dropwise to a solution of the conjugated polymer **P1** (100 mg, 0.08 mmol) in dichloromethane (100 mL). The resulting suspension was stirred for 2 days at room temperature and a nitrogen stream was bubbled through the mixture throughout the entire reaction. The reaction was quenched with methanol (50 mL). The black precipitate was filtered, washed with methanol followed by CH_2Cl_2 and dried under vacuum (90 mg, yield = 90%). The extremely low solubility of **P3** in standard solvents did not allow the characterization of the compound by NMR and GPC analyses. IR (KBr): 3078 cm^{-1} and 3020 cm^{-1} (Ar–H stretch), 2951 cm^{-1}, 2920 cm^{-1} and 2850 cm^{-1} (C–H stretch), 1577 cm^{-1} and 1458 cm^{-1} (C=C stretch in Ar), 783 cm^{-1}, 763 cm^{-1}, 744 cm^{-1}.

Synthesis of poly[4′-(5,7-(4,4-diphenyl)biphenyl)] hexabenzocoronene-*alt*-2,7-(9,9-dioctylfluorene) (P4) *via* cyclodehydrogenation

The title compound (**P4**) was prepared in a manner analogous to the procedure of **P3** to obtain the product as black powders (yield = 65%). (87 mg, yield = 88%) IR (KBr): 3080 cm^{-1}, 3057 cm^{-1} and 3026 cm^{-1} (Ar–H stretch), 2949 cm^{-1}, 2920 cm^{-1} and 2848 cm^{-1} (C–H stretch), 1583 cm^{-1} and 1500 cm^{-1} (C=C stretch in Ar), 783 cm^{-1}, 763 cm^{-1}, 740 cm^{-1}. The extremely low solubility of **P4** in standard solvents did not allow the characterization of the compound by NMR and GPC analyses.

Dispersion preparation of HBC derivatives

All dispersions were prepared by bath sonication using a Branson 5510 with a frequency of 42 kHz and a power output of 135 W. The solvent was added to a 7 mL capacity vial with several milligrams of HBC derivatives at a concentration of 0.1 mg mL^{-1} followed by sonication for 10 minutes (these samples were not centrifuged to maintain a known concentration). The mixtures were left to settle for 48 h and then dispersions were characterized by UV-Vis absorption spectra, PL spectra and PLE maps.

Results and discussion

Synthesis of the monomer and the conjugated polymer

A (4-bromophenyl)pentaphenylbenzene (**1**) was synthesized *via* a Diels–Alder reaction with tetraphenylcyclopentadienone and 4-bromotolan using Pd(0)-catalyzed Sonogashira coupling of 1-bromo-4-iodobenzene and phenylacetylene.[16] The bromo group of **1** was substituted by a pinacolboronic ester through lithiation with *n*-butyllithium in THF followed by nucleophilic substitution with 2-isopropoxy-4,4,5,5-tetramethyl[1,3,2]dioxa-

borolane to obtain the monosubstituted hexaphenylbenzene (2). One of the bromo substituents on 1,3,5-tribromobenzene or 1,3,5-tri(4-bromophenyl)benzene was subsequently substituted by a hexaphenylbenzene moiety through Suzuki coupling with **2** to give the dibromo monomer **M1** or **M2**, respectively. The **M1** and **M2** monomers were polymerized with a 9,9-dioctylfluorene-2,7-diboronic acid bis(1,3-propanediol) ester by Suzuki coupling to generate the HPB-containing conjugated polymers **P1** and **P2**. The resulting polymers are grey fibrous solids and are readily soluble in various organic solvents such as NMP, THF, toluene or CH_2Cl_2 at room temperature (25 °C). **P1** and **P2** possessed excellent organo-solubility due to the incorporation of the noncoplanar structure of HPB and fluorenes as well as aliphatic alkyl chains.[18] The chemical structures of the monomers **M1** and **M2** as well as the polymers **P1** and **P2** were confirmed by ^{1}H- and ^{13}C-NMR spectra shown in the ESI (Fig. S1–S5†), indicating that the HPB-containing polymers were successfully prepared.

Cyclodehydrogenation

The hexa-*peri*-hexabenzocoronene (HBC)-containing conjugated polymers **P3** and **P4** were synthesized by oxidative cyclodehydrogenation of **P1** and **P2**, respectively (Scheme 2). Iron(III) chloride is widely used for oxidative C–C coupling reactions as reported by Sarhan and Bolm.[19] **P1** and **P2** with hexaphenylbenzenes (HPB) moieties were therefore efficiently transformed into **P3** and **P4**, respectively, with hexa-*peri*-hexabenzocoronenes (HBC) through the use of a solution of $FeCl_3$ in nitromethane. The solution-state characterization of insoluble **P3** and **P4** is limited due to the strong π–π interaction in HBCs. The MALDI-TOF MS spectrum of the model compound **M3** which was prepared from **M2** (Scheme S1†) is shown in Fig. S6.† The isotopic distribution of **M3** was consistent with the simulated results, indicating an exact loss of twelve hydrogen atoms during intramolecular cyclodehydrogenation. Dilute dispersions of HBC-containing compounds were prepared by bath sonication for the optical investigations.

Basic characterization

Fourier transform infrared (FT-IR) spectroscopy analysis is a form of vibrational spectroscopy that is commonly used for the solid-state characterization of HPB and HBC derivatives.[20,21] As shown in Fig. 1(a) and (b), the HPB-containing compounds **P1** and **P2** exhibited IR bands of 4046 cm^{-1} and 4042 cm^{-1}, respectively, resulting from the free phenyl rings, which are potentially characteristic of non-condensed benzene rings. These bands were not observed in **P3** and **P4** due to the fused benzene ring structure of HBCs. In fingerprint bands, the five adjacent C–H groups of monosubstituted benzene on HPB underwent out-of-plane C–H deformation at 698 cm^{-1} in **P1** as well as at 696 cm^{-1} in **P2**. In contrast, **P3** and **P4** possessed several peaks at 744, 763, and 783 cm^{-1} and at 740, 763, 783 cm^{-1}, respectively, as shown in Fig. 1(c) and (d), corresponding to the C–H deformation vibration of the HBC moiety. Therefore, the FT-IR spectra of the cyclodehydrogenated compounds confirm the vibration features of the HBC units. The peaks at 698 cm^{-1} disappeared, which supports the complete cyclodehydrogenation of HPB-containing precursors into HBC-containing products.

Fig. 2 shows the thermal properties of the conjugated polymers **P1–P4** as determined by differential scanning calorimetry

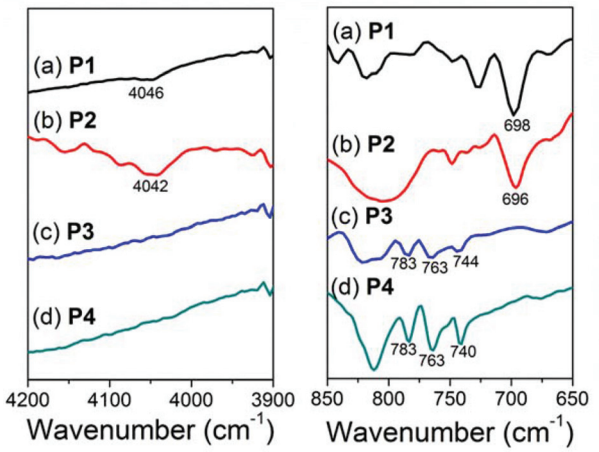

Fig. 1 FT-IR spectra of HPB-containing compounds (a) **P1** and (b) **P2** and HBC-containing compounds (c) **P3** and (d) **P4**.

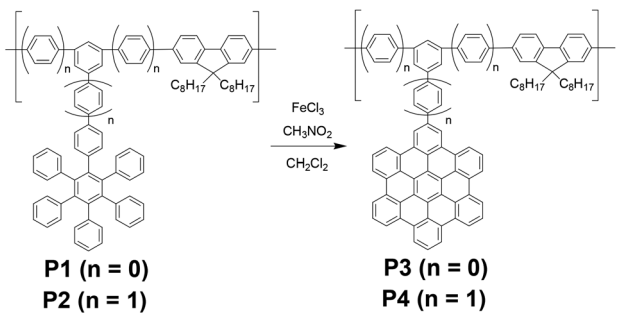

Scheme 2 Synthesis of HBC-containing conjugated polymers **P3** and **P4** *via* oxidative cyclodehydrogenation.

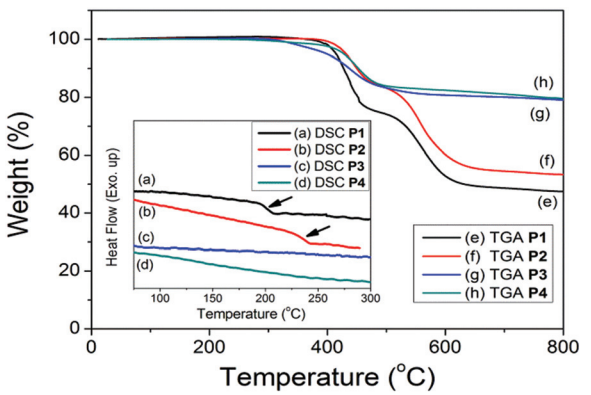

Fig. 2 DSC curves of the conjugated polymers **P1–P4** and TGA curves of **P1–P4** at a heating rate of 10 K min^{-1} under a nitrogen flow.

Table 1 Thermal properties of conjugated polymers **P1–P4**

Polymer	T_g [a] (°C)	T_{d10} [b] (°C) in N_2	in air	Char yield[c] (%)
P1	202	427		47
P2	235	449		53
P3	>300	437		79
P4	>300	453		80

[a] Glass transition temperatures (T_gs) were determined by DSC at a heating rate of 10 K min^{-1}. [b] Decomposition temperatures at 10% weight loss (T_{d10}) were measured by TGA at a heating rate of 10 K min^{-1}. [c] Residual weight percentage at 800 °C under a nitrogen flow.

(DSC) and thermogravimetric analysis (TGA). The results are summarized in Table 1. As depicted in Fig. 2, **P1** and **P2** possess high glass transition temperatures (T_gs) of approximately 202 and 235 °C, respectively. Compared to **P1**, the rigidity of **P2** backbones was enhanced by the triphenylbenzene moiety, leading to a higher T_g. In addition, the phase transition of HBC-containing **P3** and **P4** could not be observed in the region between room temperature and 300 °C, indicating that **P3** and **P4** exhibited excellent thermal stability caused by π–π interactions among HBCs. In the TGA curve, all polymers **P1–P4** showed no obvious weight loss at temperatures up to 300 °C under a nitrogen atmosphere. The temperatures required for 10% weight loss (T_{d10}) of **P3** and **P4** were slightly higher than that for **P1** and **P2**, respectively, indicating that HBCs are more thermostable than HPB. The similar degradation patterns of **P1–P4** at approximately 400 °C were attributed to the decomposition of aliphatic alkyl chains attached to the fluorene moiety. However, HBC-containing **P3** and **P4** exhibited significantly higher char yields compared to HPB-containing **P1** and **P2**. This phenomenon results from further carbonization or graphitization of HBCs and leads to an increased yield of charred residue.[22] Therefore, the incorporation of HBCs into conjugated polymers dramatically enhances the glass transition temperature and decomposition temperature, which are the desirable properties for polymers used in optoelectronic applications.

The powder X-ray diffractograms (XRD) of the conjugated polymers **P1–P4** are shown in Fig. 3. Broad amorphous halos (2 theta from 10° to 30°) were observed in **P1–P4** attributed to the disordered aliphatic alkyl chains on the fluorene moiety. The orders of **P1** and **P2** were lower than **P3** and **P4** due to the stacking hindrance caused by the noncoplanar structure of HPB.

Cyclodehydrogenated **P3** and **P4** exhibited a *d*-spacing of 1.26 and 1.37 nm, respectively, associated with the interlayer distance being dependent on the HBC size. In addition, the π–π stacking distance (3.4–3.7 Å) in planar polycyclic aromatic hydrocarbons was also observed in **P3** and **P4**. Based on the XRD spectra, the *d*-spacings of the HBC moieties on **P3** and **P4** were slightly smaller than the 15 Å spacing of HBCs ascribed to a possible tilted arrangement of the HBC moieties. Thus, the XRD results of **P3** and **P4** show a highly efficient transformation from HPB to HBCs through complete cyclodehydrogenation.

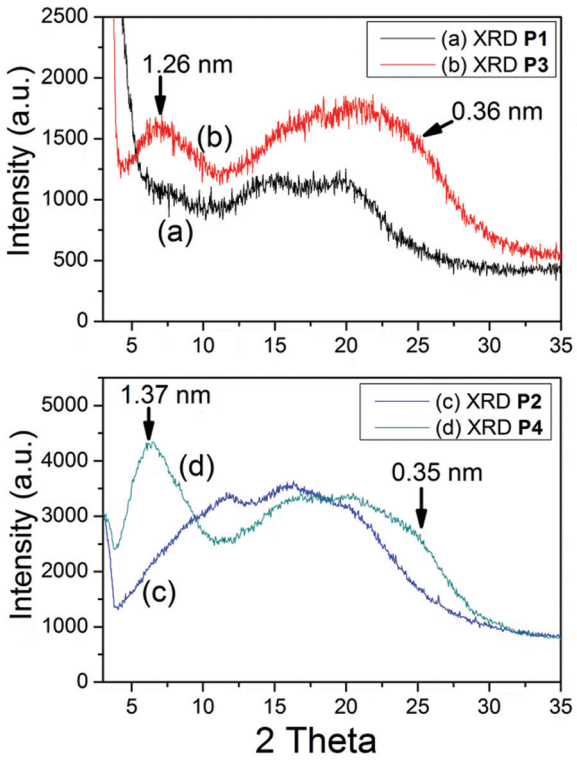

Fig. 3 Powder X-ray diffraction of conjugated polymers (a) **P1**, (b) **P3**, (c) **P2** and (b) **P4**.

Optical properties of HPB-containing P1 and P2

Fig. 4 shows the UV-Vis absorption and PL spectra of HPB-containing conjugated polymers **P1** and **P2** in THF solution (10^{-5} M). As shown in Fig. 4(a) and (b), both **P1** and **P2** exhibited shoulder absorption bands approximately at 310 nm caused by the π–π* transition of polyphenyl groups such as quarterphenyl or pentaphenyl.[23] In addition, the conjugated polymers **P1** and **P2** showed absorbance at 332 and 341 nm, respectively, attributed to the π–π* transition of the polymer backbones.[24]

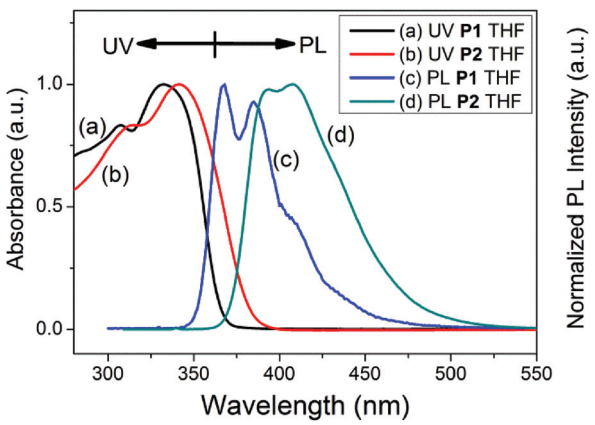

Fig. 4 UV-Vis absorption of (a) **P1** and (b) **P2** as well as PL spectra of (c) **P1** and (d) **P2** in THF solution (10^{-5} M).

Compared to **P1**, the red-shifted phenomenon of **P2** was observed at approximately 10 nm as shown in Fig. 4(b), ascribed to the enhancement of the conjugation length. The photoluminescence spectra of **P1** and **P2** in solution possessed maximum emission peaks at 368 and 408 nm, respectively. The bathochromic shift of the **P2** emission band was ascribed to the longer conjugation length of the backbone. **P1** and **P2** in THF possessed high fluorescence quantum yields of about 0.88 and 0.92, respectively, which were higher than the yield of 0.78 of poly(9,9-di-*n*-octylfluorene)[25] and the yield of 0.44 of triphenylbenzene and fluorene derivatives,[24] indicating that the propeller-like shape and steric bulkiness of HPB units impede intramolecular rotation and reduce the nonradiative decay of the excited state.[26]

Optical properties of HBC-containing P3 and P4

P3 and **P4** are insoluble in common organic solvents due to the strong π–π interactions among the HBC units. However, using an ultrasonic agitation technique, it was possible to obtain a dispersion of HBC derivatives in organic solvents for UV-Vis absorption and photoluminescence spectroscopy analyses. Fig. 5 shows the UV-Vis absorption and PL spectra of **P3** and **P4** dispersed in CHP. The absorption bands appearing approximately at 360 nm were termed β-bands (full symmetry allowed), and the shoulder at 427 nm was termed p-bands (partial symmetry forbidden), on the basis of Clar's nomenclature.[27] In Fig. 5(a) and (b), the β-bands of **P3** and **P4** were located at 369 nm and 361 nm, respectively. Compared to **P4**, the **P3** dispersion with a higher absorption wavelength is due to the ease of HBC π–π stacking, leading to a longer conjugation length. As mentioned by Kastler *et al.*, the intensities of the aggregate emissions of the alkylated HBCs increase with their increasing concentration in organic media. Therefore, the PL spectra could be regarded as secondary measurement of the aggregation phenomena of the HBCs. As shown in Fig. 5(c), **P3** revealed broad emission bands at 466, 534 and 636 nm. The emission bands beyond 600 nm were caused by aggregation of the HBC moiety, indicating that **P3** could not be well dispersed in CHP.[13] In contrast, **P4** shows resolved emission peaks at 466, 485, 495, 519 and 529 nm attributed to the photoluminescence of completely exfoliated and disaggregated HBCs. In addition, the emission bands beyond 600 nm were not observed, indicating that the **P4** polymer existed individually in CHP.

Fig. 6 displays the UV-Vis absorption spectra of conjugated polymer **P3** and **P4** dispersions in THF. As shown in Fig. 6(a) and (b), **P3** and **P4** showed transitions at 371 nm and 365 nm, respectively. The p-band absorbance (~427 nm) increased with increasing concentrations of **P4** in THF (Fig. S7†), resulting from the aggregation of HBC units at high dispersion concentrations. Therefore, the dispersion of **P3** and **P4** in different solvents could be determined by the intensity ratio $(A_{max}/A_{427})_{Ind}$ of β-bands at ~360 nm (associated with the presence of exfoliated molecules) to p-bands at ~427 nm (associated with the presence of aggregated HBCs). Here "Ind" indicates individual. The ratio $(A_{max}/A_{427})_{Ind}$ reflects the relative content of the exfoliated HBC-containing **P3** and **P4**. When the individual population is high, the ratio will increase due to lower levels of aggregation. As tabulated in Table 2, **P3** possessed $(A_{max}/A_{427})_{Ind}$ ratios of 1.96 and 1.51 in CHP and THF, respectively. On the other hand, **P4** exhibited $(A_{max}/A_{427})_{Ind}$ ratios of 4.47 and 1.76 in CHP and THF, respectively. Compared to THF as a dispersant, CHP is an excellent solvent for the dispersion of HBC-containing **P3** and **P4** due to its large $(A_{max}/A_{427})_{Ind}$ ratio. This feature could be a result of the similar Hildebrand solubility parameters of both HBC and CHP, approximately 21 $MPa^{1/2}$, which results in good dissolution and a low enthalpy of mixing between the solute and the solvent.[14] It is noteworthy that **P4** showed a higher dispersibility than **P3**, resulting from the triphenylbenzene moiety possessing more free volume for solvent penetration and steric hindrance for HBC stacking. As shown in Fig. 6(c), **P3** shows an intensive emission band at 659 nm due to the aggregation of HBC groups. Compared to **P3** in Fig. 6(c), the **P4** dispersion exhibited resolved peaks in the region between 450 and

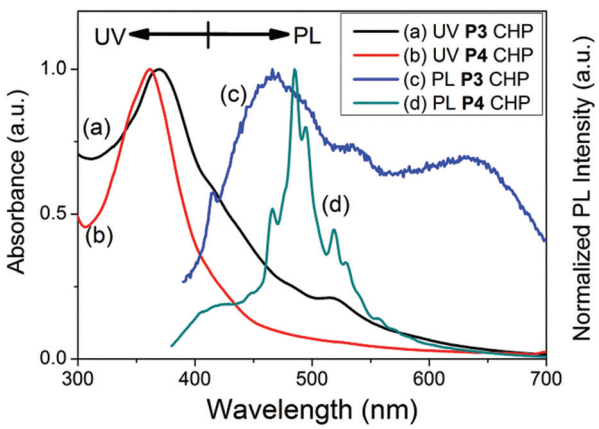

Fig. 5 (a) UV-Vis absorption spectra of (a) **P3** and (b) **P4** as well as PL spectra of (c) **P3** excited at 369 nm and (d) **P4** excited at 361 nm (0.1 mg mL^{-1}) in CHP.

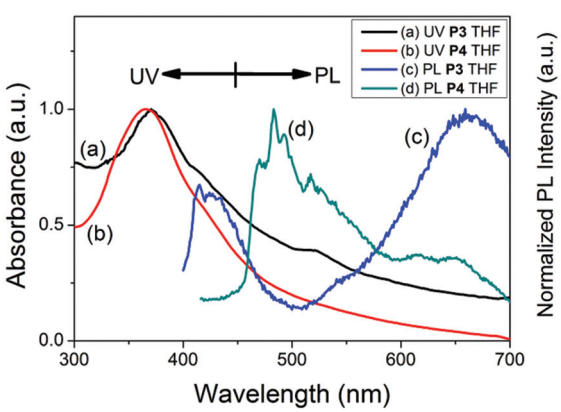

Fig. 6 (a) UV-Vis absorption spectra of (a) **P3** and (b) **P4** as well as PL spectra of (c) **P3** excited at 371 nm and (d) **P4** excited at 365 nm (0.1 mg mL^{-1}) in THF.

Table 2 Optical properties of **P3** and **P4** dispersed in different solvents

	Dispersion λ (nm)			
Polymer	Solvent	Abs. max.	PL[b]	$(A_{max}/A_{427})_{Ind}$[c]
P3	CHP	369 (0.216)[a]	466, 534, 636	1.96
P4	CHP	361 (0.254)[a]	466, 485, 495, 519, 529	4.47
P3	THF	371 (0.067)[a]	416, 659	1.51
P4	THF	365 (0.198)[a]	470, 483, 493, 517, 526, 616, 651	1.76

[a] The absorbance value of dispersions (0.1 mg mL^{-1}) from the UV-Vis spectra. [b] The excitation wavelength was at Abs. max. of the dispersions. [c] The ratio of absorbance at Abs. max. to absorbance at 427 nm for the exfoliation of **P3** and **P4**.

550 nm and weak bands beyond 600 nm in Fig. 6(d), indicating that **P4** was still well exfoliated in THF.

Fig. 7 shows the photoluminescence-excitation (PLE) maps of HBC-containing conjugated polymer **P3** and **P4** dispersions. While **P3** dispersed in CHP and THF as shown in Fig. 7(a) and (b), the unresolved emission bands were observed at 450 nm and 650 nm, respectively. The broad emission bands appeared (λ_{em} > 600 nm and λ_{ex} ~ 350–380 nm) attributed to the aggregation of HBC moieties, indicating that **P3** could not be exfoliated in solvents. As shown in Fig. 7(c), **P4** dispersed in CHP exhibited an emission–excitation region at 495 nm excited by 361 nm (*i.e.*, β-transition) and emission bands above 600 nm were not observed, which could be considered a result of the individual emissions of the HBC units, indicating that **P4** was well dispersed in CHP. When **P4** was dispersed in THF, as shown in Fig. 7(d), some weak and broad emission bands appeared (λ_{em} > 600 nm and λ_{ex} ~ 350–370 nm), which can be attributed to excimer-like emissions from few aggregated HBC units. In comparison with **P3** dispersion, **P4** dispersed well in organic solvents without significant aggregation. Due to the noncoplanar and bulky triphenylbenzene of **P4** backbones, π–π interactions among the HBC moieties were slightly hindered. In addition, no precipitation of **P3** and **P4** dispersions was observed over several days indicating the long time stability of the dispersions.

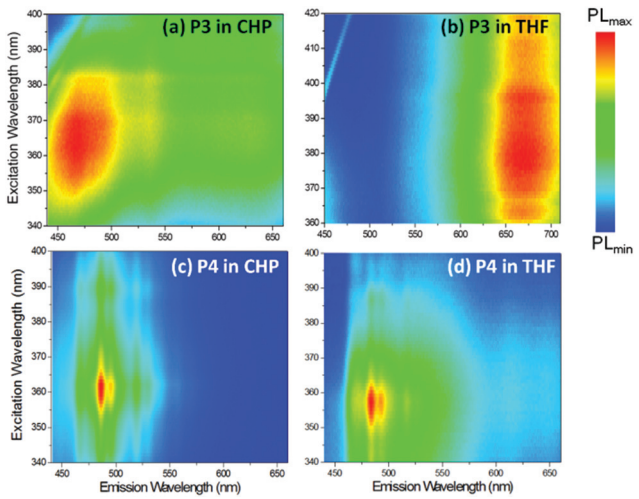

Fig. 7 Excitation–emission maps of dispersion (0.1 mg mL^{-1}) with HBC-containing **P3** in (a) CHP, (b) THF as well as **P4** in (c) CHP and (d) THF.

Conclusions

In summary, novel HPB-containing polymers (**P1** and **P2**) and nanographene-containing polymers (**P3** and **P4**) were successfully synthesized *via* Suzuki coupling and cyclodehydrogenation, respectively. The exfoliation of HBC-containing conjugated polymers **P3** and **P4** was carried out in organic solvents prepared by sonication to obtain stable and high quality dispersions. Compared to **P3** dispersion, the incorporation of triphenylbenzene into **P4** backbones showed better dispersibility in organic solvents. Therefore, the dispersion of **P4** can be considered as a prototype for the exfoliation of graphene-containing polymers and can be used for further optoelectronic applications.

Acknowledgements

The authors would like to thank the Ministry of Science and Technology (MOST) of Taiwan for the financial support for this work.

Notes and references

1 K. S. Novoselov, A. K. Geim, S. V. Morozov, D. Jiang, Y. Zhang, S. V. Dubonos, I. V. Grigorieva and A. A. Firsov, *Science*, 2004, **306**, 666–669.
2 A. K. Geim and K. S. Novoselov, *Nat. Mater.*, 2007, **6**, 183–191.
3 M. J. Allen, V. C. Tung and R. B. Kaner, *Chem. Rev.*, 2010, **110**, 132–145.
4 R. Rieger and K. Müllen, *J. Phys. Org. Chem.*, 2010, **23**, 315–325.
5 A. Narita, X.-Y. Wang, X. Feng and K. Mullen, *Chem. Soc. Rev.*, 2015, **44**, 6616–6643.
6 M. Müller, C. Kübel and K. Müllen, *Chem. – Eur. J.*, 1998, **4**, 2099–2109.
7 J. Wu, W. Pisula and K. Müllen, *Chem. Rev.*, 2007, **107**, 718–747.
8 C.-y. Liu, A. Fechtenkötter, M. D. Watson, K. Müllen and A. J. Bard, *Chem. Mater.*, 2003, **15**, 124–130.

9 A. M. van de Craats, N. Stutzmann, O. Bunk, M. M. Nielsen, M. Watson, K. Müllen, H. D. Chanzy, H. Sirringhaus and R. H. Friend, *Adv. Mater.*, 2003, **15**, 495–499.
10 J. Wu, A. C. Grimsdale and K. Mullen, *J. Mater. Chem.*, 2005, **15**, 41–52.
11 J. M. Warman, J. Piris, W. Pisula, M. Kastler, D. Wasserfallen and K. Müllen, *J. Am. Chem. Soc.*, 2005, **127**, 14257–14262.
12 W. W. H. Wong, T. B. Singh, D. Vak, W. Pisula, C. Yan, X. Feng, E. L. Williams, K. L. Chan, Q. Mao, D. J. Jones, C.-Q. Ma, K. Müllen, P. Bäuerle and A. B. Holmes, *Adv. Funct. Mater.*, 2010, **20**, 927–938.
13 J. M. Englert, F. Hauke, X. Feng, K. Mullen and A. Hirsch, *Chem. Commun.*, 2010, **46**, 9194–9196.
14 J. M. Hughes, Y. Hernandez, D. Aherne, L. Doessel, K. Müllen, B. Moreton, T. W. White, C. Partridge, G. Costantini, A. Shmeliov, M. Shannon, V. Nicolosi and J. N. Coleman, *J. Am. Chem. Soc.*, 2012, **134**, 12168–12179.
15 Y. Hernandez, V. Nicolosi, M. Lotya, F. M. Blighe, Z. Sun, S. De, I. T. McGovern, B. Holland, M. Byrne, Y. K. Gun'Ko, J. J. Boland, P. Niraj, G. Duesberg, S. Krishnamurthy, R. Goodhue, J. Hutchison, V. Scardaci, A. C. Ferrari and J. N. Coleman, *Nat. Nano*, 2008, **3**, 563–568.
16 C. Kübel, S.-L. Chen and K. Müllen, *Macromolecules*, 1998, **31**, 6014–6021.
17 I. A. Khotina, O. E. Shmakova, D. Y. Baranova, N. S. Burenkova, A. A. Gurskaja, P. M. Valetsky and L. M. Bronstein, *Macromolecules*, 2003, **36**, 8353–8360.
18 D.-J. Liaw, F.-C. Chang, M.-k. Leung, M.-Y. Chou and K. Muellen, *Macromolecules*, 2005, **38**, 4024–4029.
19 A. A. O. Sarhan and C. Bolm, *Chem. Soc. Rev.*, 2009, **38**, 2730–2744.
20 A. Centrone, L. Brambilla, T. Renouard, L. Gherghel, C. Mathis, K. Müllen and G. Zerbi, *Carbon*, 2005, **43**, 1593–1609.
21 M. G. Schwab, A. Narita, Y. Hernandez, T. Balandina, K. S. Mali, S. De Feyter, X. Feng and K. Müllen, *J. Am. Chem. Soc.*, 2012, **134**, 18169–18172.
22 F. Cataldo, O. Ursini, G. Angelini and S. Iglesias-Groth, *Fullerenes, Nanotubes, Carbon Nanostruct.*, 2011, **19**, 713–725.
23 X. Lu, C. He, P. Liu and A. C. Griffin, *J. Polym. Sci., Part A: Polym. Chem.*, 2005, **43**, 3394–3402.
24 X. Wu, H. Li, Y. Xu, H. Tong and L. Wang, *Polym. Chem.*, 2015, **6**, 2305–2311.
25 C. Xia and R. C. Advincula, *Macromolecules*, 2001, **34**, 5854–5859.
26 R. Hu, J. W. Y. Lam, Y. Liu, X. Zhang and B. Z. Tang, *Chem. – Eur. J.*, 2013, **19**, 5617–5624.
27 G. Rouillé, M. Steglich, F. Huisken, T. Henning and K. Müllen, *J. Chem. Phys.*, 2009, **131**, 204311.